

# Magnetoconductance at the 2D MIT: Evidence for Micro-Emulsion Phases

Shiqi Li, Qing Zhang, Pouyan Ghaemi, and M. P. Sarachik

Department of Physics, City College of New York, CUNY, New York, New York 10031, USA

(Dated: November 14, 2018)

Measurements of the in-plane magnetic field  $B_{sat}$  required to achieve full polarization of the electron spins in the strongly interacting two-dimensional electron system in a silicon MOSFET (Metal-Oxide-Semiconductor-Field-Effect Transistor) reveal the occurrence of a phase transition at a well-defined critical electron density for the metal-insulator transition determined from resistivity measurements. The behavior of  $B_{sat}$  as a function of electron density is consistent with the presence of the mixed electronic micro-emulsion phases proposed by Spivak and Kivelson [1].

PACS numbers:

Based on the famous 1979 paper by Abrahams, Anderson, Licciardello and Ramakrishnan [2], as well as several carefully executed experiments on different materials, it was assumed for many years that no metallic phase can exist and a metal-insulator transition (MIT) does not occur in a two-dimensional electron/hole system. It was therefore a surprise when experimental studies in the 1990's appeared to show that such a transition does take place in low disorder, dilute 2D electron systems when strong electron interactions rather than the kinetic energy are dominant and determine the behavior of the system[3]. In addition to the dramatic change in resistivity that signals the onset of a conducting phase, unusually interesting behavior was found for the magnetoresistance both above and below the critical electron density  $n_c$ . On both sides of the transition, the resistivity rises sharply with increasing in-plane magnetic field up to a field  $B_{sat}$ , above which it becomes essentially constant. Experiments [4, 5] have demonstrated that the initial increase of the magnetoresistance occurs as the magnetic field aligns the electron spins, and  $B_{sat}$  signals the onset of full spin polarization.

A great deal of discussion ensued concerning these experimental observations: is this a true metal-insulator transition, which many believed cannot occur in two dimensions, or is it a crossover that can be explained within extensions of standard Fermi liquid theory or some other relatively benign scenario. (For reviews, see Ref.[6].)

While abrupt changes and divergences have been reported at  $n_c$  for a variety of physical properties [6, 7], the benign behavior of the magnetoresistance at the critical electron density has been an enigma since its discovery [8, 9]. While the resistivity displays a sharp change as one crosses the transition at the critical density, the magnetoresistance appears to vary smoothly without exhibiting any change that would signal the onset of a new phase [10].

In this letter, we report the results of detailed measurements of the magnetoresistance of a two-dimensional low disorder, dilute, strongly interacting system of electrons in a silicon MOSFET[11]. Despite the apparent similarity of the magnetoconductance in the metallic and insulat-

ing phases, our measurements reveal the occurrence of a phase transition at a well-defined electron density  $n_k$  in the vicinity of the critical density  $n_c$  for the metal-insulator transition determined from resistivity measurements. We suggest that the behavior of  $B_{sat}$  as a function of electron density  $n_s$  is consistent with the presence of the mixed, electronic micro-emulsion phases proposed by Spivak and Kivelson [1].

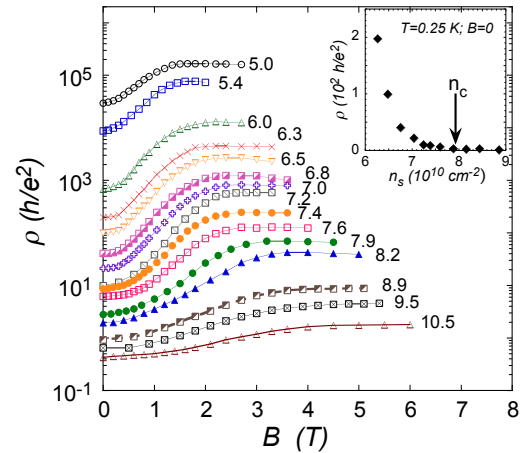


FIG. 1: The resistivity as a function of parallel magnetic field at  $T = 0.25$  K plotted on a semi-log scale for different electron densities as labelled (in units of  $10^{10} \text{ cm}^{-2}$ ). The small decrease of the resistance in some of the curves for magnetic fields above saturation is due to misalignment of the field away from the in-plane direction. To illustrate the abrupt change in the resistivity at  $n_c$ , the inset shows  $\rho$  as a function of electron density  $n_s$ .

Measurements were performed down to 0.25 K in an Oxford Heliox He-3 refrigerator on the same type of high-mobility silicon MOSFET samples as those used in previous studies [7, 12]. Here we report data taken for a sample with critical density  $n_c \approx 7.74 \times 10^{10} \text{ cm}^{-2}$  in the absence of magnetic field [13]. Contact resistance was minimized by using a split-gate geometry which permits high electron density to be maintained near the contacts independently of the value of the electron density in the main part of the sample. This is a particularly impor-

tant feature that enables reliable measurements in the dilute 2D electron system in the deeply insulating state where the resistivity reaches very high values. By contrast with the lock-in techniques that were sufficient for our earlier measurements of higher density metallic-like samples that have relatively low resistivities,[14] the measurements here were taken by a protocol similar to those described in Ref. [12], where a Keithley Source Measure Unit SMU 236 was used to apply a small DC current (as low as a few pA) through the sample and the voltage was measured by a standard four-probe method. For each density and temperature, the resistivity  $\rho$  was deduced from the slope of the linear portion of the corresponding  $I - V$  characteristic.

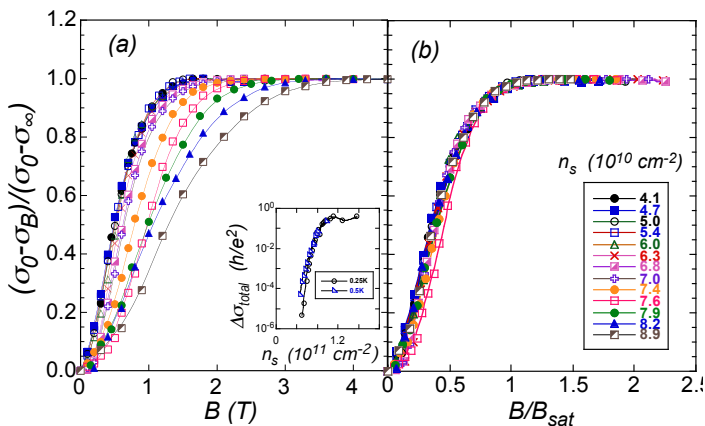


FIG. 2: Frame (a): Normalized conductivity as defined by Eq. (2) plotted as a function of in-plane magnetic field  $B$ ;  $T = 0.25$  K. The inset shows  $\Delta\sigma_{total} = [\sigma(B = 0) - \sigma(B \rightarrow \infty)]$  versus electron density  $n_s$ . Frame (b): Normalized conductivity as a function of  $B/B_{sat}$ , where the fitting parameter  $B_{sat}$  was chosen to yield a collapse of the normalized conductivity onto a single curve.

For various different electron densities, Fig. 1(a) shows the resistivity at  $T = 0.25$  K as a function of magnetic field applied parallel to the plane of the sample. In agreement with data shown in an earlier paper [10], the in-plane magnetoresistance rises dramatically with increasing magnetic field and reaches a plateau above a density-dependent field  $B_{sat}$ . The behavior of the magnetoresistance is qualitatively the same in the insulating phase as it is in the conducting phase and appears to evolve continuously and smoothly, with no indication that a transition has been crossed. As shown in the inset, this is in clear contrast with the dramatic change found for the zero-field resistance as the electron density is reduced below  $n_c$ , a change that becomes sharper and more pronounced as the temperature is reduced into the milliKelvin range.

Following the procedure used in a previous study [14],

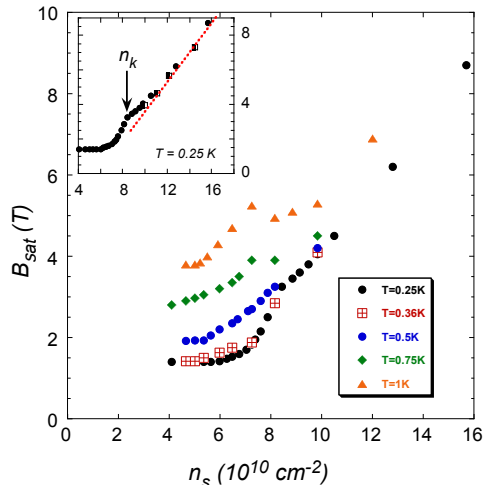


FIG. 3: The scaling parameter  $B_{sat}$  as a function of electron density for different temperatures, as labeled. The inset shows  $B_{sat}$  as a function of  $n_s$  deduced from data at the base temperature of 0.25 K. The closed circles are for the sample for which most of the data was obtained, while the half-open squares were obtained for a similar sample with a different value of  $n_c$ . To aid the discussion in the text, the dotted line is an approximate straight line fit to the high density values, extended to lower densities.

we determine the normalized magnetoconductivity:

$$\sigma_{\text{norm}} \equiv \frac{\sigma(B = 0) - \sigma(B)}{\sigma(B = 0) - \sigma(B \rightarrow \infty)} = \frac{\Delta\sigma}{\Delta\sigma_{total}}. \quad (1)$$

Note that the normalized magnetoconductivity is simply the field dependent contribution to the conductivity,  $\Delta\sigma = [\sigma(B = 0) - \sigma(B)]$ , normalized by its full value,  $\Delta\sigma_{total} = [\sigma(B = 0) - \sigma(B \rightarrow \infty)]$ .

Figure 2 (a) shows the normalized conductivity at  $T = 0.25$  K as a function of in-plane magnetic field for different electron densities. The inset is a plot of  $\Delta\sigma_{total} = [\sigma(B = 0) - \sigma(B \rightarrow \infty)]$  as a function of electron density. Notwithstanding the apparent continuity of the behavior of the magnetoconductance across the transition, the inset shows that there is a sharp change in the magnetoconductivity at the critical density  $n_c$ .

As shown in Fig. 2 (b), a density-dependent parameter  $B_{sat}$  can be chosen that provides a collapse onto a single curve for all the data shown in frame (a). The parameter  $B_{sat}$ , the in-plane magnetic field required to achieve full saturation, is shown in Fig. 3 at several different temperatures. In all cases  $B_{sat}$  decreases with decreasing electron density and assumes a constant value at very low density. A detailed understanding of the nonmonotonic behavior at different temperatures will require additional measurements. Whatever the origin of the complex behavior, it is important to note that  $B_{sat}$  is essentially the same for  $T = 0.36$  and  $0.25$  K, the two lowest measured temperatures, so that it has reached a constant value at low

temperatures as well as low densities. To aid the discussion below, the inset shows the behavior of  $B_{sat}$  deduced from data obtained at the base temperature ( $T = 0.25$  K).

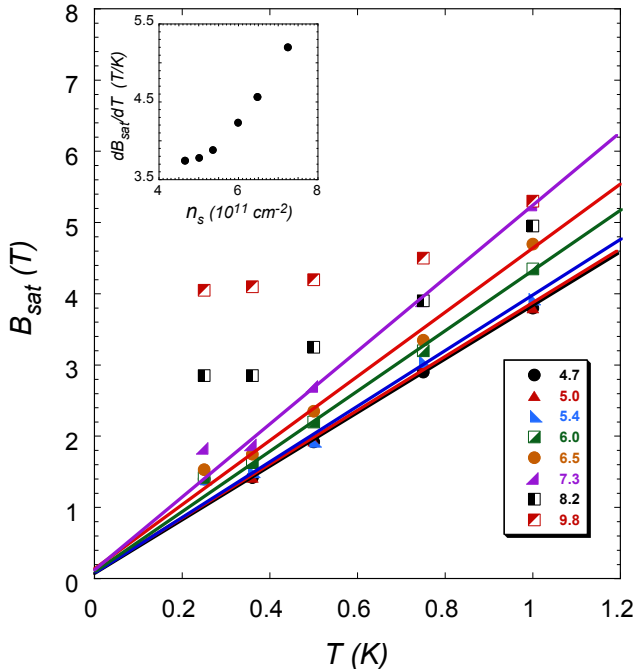


FIG. 4: The scaling parameter  $B_{sat}$  as a function of temperature  $T$ . For the six lower densities, which are insulating, the lines are linear fits to the data not including the data at the lowest temperature  $T = 0.25$  K, which lie above the curve. The upper two curves are on the metallic side of the transition. The inset shows the slope  $A$  of the  $B_{sat}$  vs.  $T$  curves in the insulating phase as a function of electron density.

Lastly, we show  $B_{sat}$  as a function of the temperature  $T$  for various different electron densities in Fig. 4. For each of the six densities on the insulating side of the transition,  $B_{sat}$  is consistent with the linear fits shown provided the values at  $T = 0.25$  K are omitted. Careful examination shows that the saturation magnetic field is the same for the two lowest temperatures and lies above the linear fits. Thus,  $B_{sat} = AT$  for temperatures above  $\approx 0.4$  K and saturates to a constant value as the temperature is further reduced. The inset shows the slope  $A$  of the straight line fits as a function of electron density. Again, the slope  $A$  decreases as the density is reduced, heading toward zero at  $T = 0$ , but levels off instead to a constant values as the density is reduced. By contrast, the behavior of  $B_{sat}$  is distinctly different for the two highest densities, signaling the entry into a different phase.

We now examine the complex and interesting behavior of  $B_{sat}$  versus  $n_s$  obtained at the lowest (base) tempera-

ture of 0.25 K, the temperature that is most stable and where the bulk of the measurements were taken (see the inset to Fig. 3). Of particular interest is the kink that occurs at density  $n_k \approx 8.4 \times 10^{10} \text{ cm}^{-2}$ , shown by the arrow. Spivak and Kivelson[1] have proposed that there exist micro-emulsion phases between the liquid and solid phases in the form of a meso-scale mixture of Fermi liquid and Wigner crystallites. Note that transport evidence for quantum electron crystallization in similar samples has recently been reported by Brussarski *et. al* [15]. As briefly described below and discussed in detail as Supplementary Material, we suggest that our results are consistent with the existence of microemulsion phases within which we have observed a percolation transition at  $n_k$ .

We have deduced the polarizability of the electron spins from transport measurements rather than from measurements of the magnetic response itself. We must therefore indicate how a determination of  $B_{sat}$  obtained from a measurements of the resistivity yields the information we seek.

For very high electron densities, above the kink denoted by the arrow in the inset to Fig. 3, the ends of the sample are connected by conduction through Fermi liquid. As the electron density is reduced toward the kink and Wigner crystallites begin to form, the conduction continues to be dominated by the properties of parallel paths through the Fermi liquid which have much higher conductance than the parallel paths through Wigner crystal regions, until the percolation limit is reached. At this point, due to the increase of the volume fraction of Wigner crystals, there no longer exists an uninterrupted path for the electrons to travel through the Fermi liquid, which have much higher conductance than the parallel paths through Wigner crystal regions.

The approach to the kink from above is consistent with what one expects as the microemulsion forms, as follows. For large electron densities, we observe the linear dependence of  $B_{sat}$  on density expected for a Fermi liquid, as shown by the dotted red line in the inset to Fig. 3. As the electron density  $n_s$  is reduced, Wigner crystals begin to form, giving rise to microemulsion phases. Since Wigner crystals have a lower density than the parent Fermi liquid, the electronic density in the remaining Fermi liquid regions will increase due to the formation of Wigner crystallites. The saturation magnetic field in the Fermi liquid is an increasing function of electronic density, and  $B_{sat}$  is thus expected to increase when Wigner crystallites emerge. Indeed, we observe an up-turn of  $B_{sat}$  away from linear behavior as we approach the kink from above (see the dotted red line in the inset to Fig. 3). We suggest that the kink signals the occurrence of a percolation transition.

For electron densities below the kink, the paths connecting the two edges through Fermi liquid regions are now blocked by Wigner crystals and the (much lower) conduction proceed by hopping conductivity [12]. At

these densities, the Fermi-liquid and Wigner crystal regions act as resistances in series, and the resistance is thus more sensitive to the areas with lower conductivity, namely the Wigner crystals.

By contrast with the conductivity above the kink, which depends overwhelmingly on the density of the Fermi liquid regions, the conductivity below the kink depends on both the Fermi liquid density and the volume fraction of the Wigner crystal component which increases with decreasing overall electron density and depends on the size of the Wigner crystallites as a function of temperature and magnetic field as governed by the Pomeranchuk effect.

As will be discussed in detail in the Supplementary Materials, the Pomeranchuk effect may be responsible for the fact that  $B_{sat}$  becomes independent of temperature at the lowest temperatures, as seen experimentally. That  $B_{sat}$  becomes a constant at very low electron densities may be due to the fact that the volume fraction of Wigner crystal has reached 100 percent, so that the limiting value of  $B_{sat}$  characterizes the pure Wigner crystal. Alternatively, it may be a measure of the disorder in our sample.

In light of the above arguments, the dependence of  $B_{sat}$  on the total electron density is through fundamentally different processes at low and high density, thereby leading to the kink at  $n_k$  shown in Fig. 3. A more detailed, quantitative analysis of these issues and their correspondence with our experimental results are presented in the section on Supplementary Materials.

To summarize, contrary to earlier reports, we have shown that the magnetoconductance exhibits critical behavior, and provides a sharp and unequivocal determination of the electron density of the metal-insulator transition in a strongly interacting electron system in two dimensions. The novel experimental protocol and analysis presented in this paper can be used to map the entire phase diagram by measuring the value of  $n_k$  as various parameters are varied, such as the temperature, magnetic field and disorder. On the basis of our data and analysis, we suggest that the behavior of the 2D electron system in silicon MOSFETs is consistent with a percolation transition within mixed, micro-emulsion phases composed of Wigner crystallites and Fermi liquid, as proposed by Spivak and Kivelson [1].

We are grateful to Teun Klapwijk for providing the split-gate geometry samples that enabled these experiments. We thank Steve Kivelson for valuable suggestions and Sergey Kravchenko for his careful reading of the manuscript. This work was supported by the National Science Foundation grant DMR-1309008 and the Binational Science Foundation Grant 2012210. PG acknowledges support by NSF EFRI-1542863 and PSC-CUNY Award, jointly funded by The Professional Staff Congress and The City University of New York.

- 
- [1] B. Spivak, Phys. Rev. B **67**, 125205 (2003); B. Spivak and S. A. Kivelson, PRB **70** 155114 (2004); Annals of Phys. **321**, 2071-2115 (2006).
  - [2] E. Abrahams, P. W. Anderson, D. C. Licciardello, and T. V. Ramakrishnan, Phys. Rev. Lett. **42**, 673 (1979).
  - [3] S. V. Kravchenko, G. V. Kravchenko, J. E. Furneaux, V. M. Pudalov, and M. D'Iorio, Phys. Rev. B **50**, 8039 (1994); S. V. Kravchenko, W. E. Mason, G. E. Bowker, J. E. Furneaux, V. M. Pudalov, and M. D'Iorio, Phys. Rev. B **51**, 7038 (1995); S. V. Kravchenko, D. Simonian, M. P. Sarachik, Whitney Mason, and J. E. Furneaux, Phys. Rev. Lett. **77**, 4938 (1996).
  - [4] T. Okamoto, K. Hosoya, S. Kawaji, and A. Yagi, Phys. Rev. Lett. **82**, 3875 (1999).
  - [5] S. A. Vitkalov, H. Zheng, K. M. Mertes, M. P. Sarachik, and T. M. Klapwijk, Phys. Rev. Lett. **85**, 2164 (2000); S. A. Vitkalov, M. P. Sarachik, and T. M. Klapwijk, Phys. Rev. B **64**, 073101 (2001).
  - [6] For reviews see: E. Abrahams, S. V. Kravchenko and M. P. Sarachik, Rev. Mod. Phys. **73**, 251 (2001); S. V. Kravchenko and M. P. Sarachik, Rep. Prog. Phys. **67**, 1 (2004); B. Spivak, S. V. Kravchenko S. A. Kivelson, and X. P. A. Gao, Rev. Mod. Phys. **82**, 1743 (2010).
  - [7] A. Mokashi, S. Li, B. Wen, S. V. Kravchenko, A. A. Shashkin, V. T. Dolgoplov, and M. P. Sarachik, Phys. Rev. Lett. **109**, 096405 (2012).
  - [8] D. Simonian, S. V. Kravchenko, M. P. Sarachik and V. M. Pudalov, Phys. Rev. Lett. **79**, 2304 (1997).
  - [9] V. M. Pudalov, G. Brunthaler, A. Prinz and G. Bauer, JETP Lett. **65**, 932 (1997).
  - [10] K. M. Mertes, D. Simonian, M. P. Sarachik, S. V. Kravchenko and T. M. Klapwijk, Phys. Rev. B **60** R5093 (1999).
  - [11] This follows earlier work by our group that focused largely on metallic electron densities. See Yeekin Tsui, S. A. Vitkalov, M. P. Sarachik and T. M. Klapwijk, Phys Rev B **71**, 033312 (2005).
  - [12] Shiqi Li, and M. P. Sarachik, Phys. Rev. B **95**, 041301(R) (2017).
  - [13] The critical density has been shown to be a weak function of magnetic field. See Kevin Eng, X. G. Feng, Dragana Popovic and S. Washburn, Phys. Rev. Lett. **88** 136402 (2002); A. A. Shashkin, S. V. Kravchenko, V. T. Dolgoplov and T. M. Klapwijk, Phys Rev. Lett. **87**, 266402 (2001).
  - [14] S. A. Vitkalov, H. Zheng, K. M. Mertes, and M. P. Sarachik, Phys. Rev. Lett. **87**, 086401 (2001).
  - [15] P. Brussarski, S. Li, S. V. Kravchenko, A. A. Shashkin and M. P. Sarachik, Nature Comm. **9** 3803 (2018).

## Supplementary materials: Magnetoconductance at the 2D MIT: Evidence for Micro-Emulsion Phases

From measurements of the magnetic field dependence of the resistivity, we claim that a phase transition occurs at a critical electron density  $n_k$  where a kink occurs in the magnetic field  $B_{sat}$  required to fully polarize the electron spins. In order to understand the origin of the kink in  $B_{sat}$  versus the total density  $n_s$ , we need to examine the nature of the conductivity over the entire range of electron densities, both above and below the kink.

Given the definition of the normalized conductivity, repeated below:

$$\sigma_{norm}(B) \equiv \frac{\sigma(B=0) - \sigma(B)}{\sigma(B=0) - \sigma(B \rightarrow \infty)} = \frac{\Delta\sigma}{\Delta\sigma_{total}}. \quad (2)$$

The saturation magnetic field corresponds to the field where  $\sigma_{norm}(B_{sat}) = 0.99$ .

In a microemulsion phase consisting of insulating Wigner crystals and conducting Fermi liquid, the conductivity of the sample depends on the geometry of the Wigner and Fermi regions. Many techniques have been used to calculate the conductivity of composite conductors [1]. Here we present a simplified model which can capture the essential effect of the geometry of the crystalline and liquid regions on the measured saturation field. We consider the sample to be a rectangle with width  $D$  perpendicular to the direction of the current and length  $L$  along the direction of current. We assume the effective length of the Fermi liquid and Wigner crystal regions to be  $l_F$  and  $l_W$  and their effective width to be  $d_F$  and  $d_W$ , respectively.

At large densities,  $B_{sat}$  decreases linearly with the decrease of density, the behavior expected for a Fermi liquid. As the density is decreased toward  $n_k$ , the Wigner crystal regions start to emerge in the parent Fermi liquid. The Wigner crystal regions have insulating behavior but the sample presents conducting behavior so long as the Fermi liquid regions are large enough to percolate between the two edges. Assuming that the length of the Fermi and Wigner regions are of the order of the sample length, the conductance is through parallel Fermi liquid and Wigner crystal regions connecting the two ends of the sample. The effective conductivity of the sample will be then:

$$\sigma = \sigma_F \frac{d_F}{D} + \sigma_W \frac{d_W}{D} \quad (3)$$

where  $\sigma_W$  and  $\sigma_F$  are the conductance of Wigner crystal and Fermi liquid, respectively. Since  $\sigma_W \ll \sigma_F$ , and assuming that for densities above  $n_k$  the Wigner crystal regions are not much larger than Fermi-liquid regions ( $d_w \gg d_F$ ), Eq. (3) gives  $\sigma \approx \sigma_F \frac{d_F}{D}$  and the normalized conductivity in equation (2) reads:

$$\sigma_{norm}(B) \approx \frac{\Delta\sigma_F}{\Delta\sigma_{F,Total}} = \sigma_{norm}^F(B). \quad (4)$$

Thus, for densities above  $n_k$ , the saturation magnetic field corresponds to that of the Fermi liquid. It is important to understand how the emergence of Wigner crystal regions affect the density in the remaining Fermi liquid. Since Wigner crystals have a lower density than the parent Fermi liquid, their formation causes the density of the remaining liquid to increase, with a consequent deviation of  $B_{sat}$  upward from straight line behavior as the kink is approached from above. Figure 1 shows such a decrease of the slope of  $B_{sat}$  versus total density  $n_s$  as the density is decreased toward the kink.

As the density is decreased further, the fraction of the Wigner crystal regions increases and, ultimately, there will be no path through the Fermi liquid regions to connect the two edges of the sample. We suggest that the appearance of the kink at the density  $n_k$  corresponds to a percolation transition. At densities below  $n_k$ , the paths connecting the two edges of the sample pass through Wigner crystal and Fermi liquid regions in series. The effective conductivity of the sample is then given by:

$$\sigma = \frac{L}{D} \frac{\sigma_F \sigma_W d_F}{\sigma_F l_W + \sigma_W l_F}. \quad (5)$$

As the Wigner crystal and Fermi liquid regions are in series their effective lengths cover the length of sample i.e.  $L = l_W + l_F$ . The normalized conductivity is then

$$\sigma_{norm}(B) = \frac{\frac{\sigma_W(0)}{\frac{\sigma_W(0)}{\sigma_F(0)} + \frac{l_W(0)}{l_F(0)}} - \frac{\sigma_W(B)}{\frac{\sigma_W(B)}{\sigma_F(B)} + \frac{l_W(B)}{l_F(B)}}}{\frac{\sigma_W(0)}{\frac{\sigma_W(0)}{\sigma_F(0)} + \frac{l_W(0)}{l_F(0)}} - \frac{\sigma_W(\infty)}{\frac{\sigma_W(\infty)}{\sigma_F(\infty)} + \frac{l_W(\infty)}{l_F(\infty)}}}. \quad (6)$$

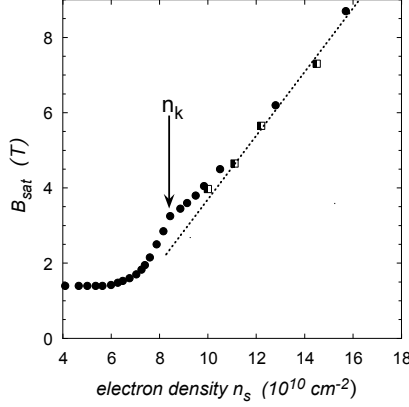


FIG. 1: The scaling parameter  $B_{sat}$  as a function of electron density at  $T = 0.25$  K. The closed circles and half open squares refer to two samples with different critical densities as determined from resistivity measurements. The dotted line is an approximate straight line fit to the high density values, extended to lower densities.

Notice that due to the Pomeranchuk effect the Wigner crystal fraction over the sample depends on in-plane magnetic field [2]. The dependence is explicitly presented in equation (6) as  $\frac{l_W}{l_F}(B)$ .

To understand the kink in  $B_{sat}$  versus total density  $n_s$  curve, we need to examine the conductivity given by Eq. (6) for densities slightly smaller than the kink. In this case, the size of Wigner crystal is small ( $l_W \ll l_F$ ) such that  $\frac{\sigma_W}{\sigma_F} \gg \frac{l_W}{l_F}$  and the difference between the normalized conductivity of the Fermi liquid and the normalized conductivity of the whole sample is approximately:

$$\begin{aligned} \sigma_{norm}^F(B) - \sigma_{norm}(B) \approx \sigma_{norm}^F(B) & \left[ \frac{\sigma_F(0)^2 l_W}{\sigma_W(0) l_F}(0) \left( \frac{1}{\sigma_F(0) - \sigma_F(B)} - \frac{1}{\sigma_F(0) - \sigma_F(\infty)} \right) \right. \\ & \left. - \frac{\sigma_F(B)^2 l_W}{\sigma_W(B) l_F}(B) \frac{1}{\sigma_F(0) - \sigma_F(B)} + \frac{\sigma_F(\infty)^2 l_W}{\sigma_W(\infty) l_F}(\infty) \frac{1}{\sigma_F(0) - \sigma_F(\infty)} \right] \end{aligned} \quad (7)$$

It can be readily seen from Eq.(7) (or Eq.(6) for that matter) that when  $l_W \rightarrow 0$ , the normalized conductivity  $\sigma_{norm}(B)$  approaches the normalized conductivity of the fermi liquid ( $\sigma_{norm}^F(B)$ ), as was the case for densities larger than the kink density. This leads to the continuity of  $B_{sat}$  versus density at the kink density  $n_k$ .

As for the change of the slope of  $B_{sat}$  versus density at  $n_k$ , we can see from Eq.(7) that, as the density is decreased below  $n_k$ , the normalized conductivity relative to the normalized conductivity is reduced from that of the Fermi liquid.

We now show that  $\sigma_{norm}^F(B) > \sigma_{norm}(B)$ . As discussed in reference [2], at low enough temperature and for magnetic fields of the order of saturation magnetic field, the volume fraction of Wigner crystal is of the order of the volume fraction for infinite magnetic field (i.e.  $\frac{l_W}{l_F}(B_c) \approx \frac{l_W}{l_F}(\infty)$ ). Equation (7) then simplifies to:

$$\sigma_{norm}^F(B) - \sigma_{norm}(B) = \sigma_{norm}^F(B) \left[ \frac{\sigma_F(0)^2 l_W}{\sigma_W(0) l_F}(0) - \frac{\sigma_F(\infty)^2 l_W}{\sigma_W(\infty) l_F}(\infty) \right] \left[ \frac{1}{\sigma_F(0) - \sigma_F(B)} - \frac{1}{\sigma_F(0) - \sigma_F(\infty)} \right] \quad (8)$$

$\sigma_F(B)$  is a decreasing function of  $B$  and its value at  $B = 0$  is  $2\sigma_F(\infty)$ . The conductance of Wigner crystals is not sensitive to the applied magnetic field. If the magnetic field induced increase of  $l_W$  due to the Pomeranchuk

effect is not too large (i.e.  $\frac{l_W}{l_F}(\infty) < 4\frac{l_W}{l_F}(0)$ ), which we expect at least for low enough temperatures [2], the value give in Eq.(7) is positive. As a result,  $\sigma_{norm}(B) = 0.99$  is achieved at a magnetic field which is less than saturation magnetic field of Fermi liquid. This result explains the fast decrease of  $B_{sat}$  versus density at  $n_k$  which corresponds to percolation transition in microemulsion phase.

To analyze the behavior of conductivity at densities much smaller than  $n_k$ , we can use the fact that conductance of Wigner crystals is only weakly dependent on the magnetic field ( $\sigma_W(B) \approx \sigma_W(0) = \sigma_W$ ) and simplify equation (6) to:

$$\sigma_{norm}(B) \approx \frac{\frac{1}{\frac{\sigma_W}{\sigma_F(0)} + \frac{l_W}{l_F}(0)} - \frac{1}{\frac{\sigma_W}{\sigma_F(B)} + \frac{l_W}{l_F}(B)}}{\frac{1}{\frac{\sigma_W}{\sigma_F(0)} + \frac{l_W}{l_F}(0)} - \frac{1}{\frac{\sigma_W}{\sigma_F(\infty)} + \frac{l_W}{l_F}(\infty)}}. \quad (9)$$

As we decrease the density further below  $n_k$ , the length of the Wigner crystals increases (i.e.  $l_W \lll l_F$ ), while  $\sigma_W \ll \sigma_F$  regardless of the total density. As a result, we can assume that  $\frac{\sigma_W}{\sigma_F} \ll \frac{l_W}{l_F}$  and simplify equation (9) to:

$$\sigma_{norm}(B) \approx \frac{\frac{l_F}{l_W}(0) - \frac{l_F}{l_W}(B)}{\frac{l_F}{l_W}(0) - \frac{l_F}{l_W}(\infty)} \quad (10)$$

It is apparent from Eq.(10) that at densities well below the kink, the normalized conductivity is determined by the volume fraction of the Wigner crystals. The magnetic field and temperature dependence of the crystal volume fraction is mainly determined by the Pomeranchuk effect. As shown in reference [2], at low enough temperature the volume fraction becomes independent of temperature, and consequently, so do the normalized conductivity and  $B_{sat}$ , consistent with experiment.

---

[1] Scott Kirkpatrick, Rev. Mod. Phys. 45, **574**, 574-588 (1973)

[2] Boris Spivak and Steven Kivelson, Annals of Phys. **321**, 2071-2115 (2006)